METHODOLOGY DEVELOPMENT FOR HIGH STRAIN RATE DAMAGE IN LAMINATED COMPOSITE MATERIALS

G. Battams[1*], J. M. Dulieu-Barton[1], S.W. Boyd[1]

[1]*Faculty of Engineering and the Environment, University of Southampton, SO17 1BJ, UK*
**G.Battams@soton.ac.uk*

Keywords: Composites, damage, high strain rate, tensile, digital image correlation, DIC

Abstract
An experimental methodology is presented to allow the application of an interrupted high strain rate tensile load to fibre reinforced polymer (FRP) specimens. Loading is intended to initiate damage but to avoid complete specimen failure, allowing subsequent studies on the damage propagation behaviour. The use of an open loop servohydraulic test machine at high actuator velocities has required the development of a novel rig design to allow interrupted loading and to ensure pure tensile loading. The work describes the validation of the rig design at quasi-static strain rates using strain gauges and white light imaging combined with digital image correlation (DIC). The use of the rig at high strain rates is to be discussed further in the oral presentation along with the imaging of damage initiation behaviour using high frequency optical measurement techniques.

1 Introduction

Fibre reinforced polymer (FRP) materials are being used increasingly in a wide variety of industries including the aerospace, marine and automotive sectors, where the combination of their mechanical properties and durability have made them invaluable in many instances. Such applications introduce the risk of impact type events occurring; such as bird strikes, hail damage, slamming in rough seas or simply a dropped tool during maintenance [1-3]. The quasi-static behaviour of FRP materials has been studied in detail, e.g. [4], but material responses at elevated strain rates such as those developed during impact loading are less well defined [5]. The current work aims to validate a loading methodology that can apply high strain rate loads to FRP specimens without complete specimen failure. This will initiate high strain rate damage in the specimens whilst allowing subsequent testing of damage propagation behaviour under fatigue type loads to take place, mimicking the service load on the material.

The majority of previous studies on the behaviour of FRP materials at high strain rates have used split-Hopkinson pressure bar (SHPB) devices, e.g. [6]. These devices require small specimen samples of around 10 mm length in order to minimise inertia and wave-propagation effects, conflicting with the need for FRP specimens to be large relative to the reinforcement [5]. Free-edge effects are also more influential in small specimens as they generally occur within a laminates width from the specimen free edge [7]. The current research aims to establish a methodology for investigating the effect of high rate tensile loads on FRP materials using larger and consequently more representative specimen sizes.

The work by Fitoussi *et al* [8] explores the failure behaviour of FRP materials under high strain rate tensile loading. Randomly reinforced glass polyester and woven carbon epoxy laminates were subjected to high strain rate loading up to 20.5 s^{-1}. Damage was quantified using two methods, the first being a macroscopic reduction in Young's modulus derived from the load cell data and from strain gauges attached to specimens. A second damage parameter was quantified at the micro scale using a scanning electron microscope (SEM) to analyse a representative element volume. Image analysis performed on the SEM data was used to quantify the number of matrix microcracks and fibre-matrix debonds. The authors found that the strain at which damage first occurred was delayed at higher applied strain rates in both glass polyester and woven CFRP specimens. Woven CFRP specimens were found to exhibit a near homogenous distribution of damage at quasi-static strain rates, whilst loading at higher strain rates caused increasingly localised and clustered regions of damage, possibly due to the lack of time for stress redistribution at the initial areas of stress concentration. Such inhomogeneous damage behaviour was not found in glass polyester samples. The use of full-field techniques would prove beneficial over point measurement techniques where damage is found to be localised.

2 Interruptible Loading Rig Design

An Instron VHS 80/20 machine used in this work can apply a maximum load of 80 kN at an actuator velocity of 20 m/s. The VHS machine is capable of intermediate strain rates of the order 100 s^{-1} and can accept standard sized tensile specimens of up to 30 mm width. The load is measured using a Kistler 9071A, quartz type load cell, minimising the possibility of load cell ringing. The actuator is allowed to reach a constant velocity prior to any loading taking place through the use of a slack adaptor system. For these reasons, the VHS machine is the preferred method of load application for intermediate strain rate tests. The machine achieves high actuator velocities through the controlled but sudden release of hydraulic oil stored in a set of high pressure accumulators. Although a linear voltage displacement transducer (LVDT) tracks actuator displacement, a feedback loop does not exist between the LVDT and the accumulator outlet valve. Actuator velocity is instead controlled using a predefined calibration file relating accumulator valve drive voltage values against time, such that a near constant actuator velocity is achieved throughout a test. The actuator is decelerated by a buffer at the end of its travel. Since no feedback loop exists when operating at high actuator velocities, it is not possible to stop the actuator at a predetermined load or position using the standard machine setup. The high inertia of the actuator would further complicate the ability to stop at a predefined load or position. Therefore, to be able to apply a high strain rate load without total specimen failure, an additional rig is required to act as a mechanical fuse in the loading path.

The study by Fitoussi *et al* [8] used double edge notched tensile (DENT) fuses loaded in series with composite specimens to allow interrupted loading when using a Schenk servo-hydraulic test machine at actuator velocities up to 20 m/s. Polymethylmethacrylate (PMMA) DENT fuses characterised by a brittle failure behaviour were manufactured with a range of ligament widths, thus allowing interrupted loading at various load levels. A finite-element analysis (FEA) model was developed to ensure a smooth load transient into the composite specimen and to ensure homogenous stress and strain fields within the gauge length. In the present work, high frequency white-light imaging combined with digital image correlation (DIC) is used to provide full-field maps of strain, so the optimisation of fuse and rig design to achieve a homogenous strain field is less crucial.

It was decided that the manufacture of DENT fuses would be expensive and time consuming for each interrupted test. The DENT fuse design also requires the use of an extra set of grips in series with the FRP specimen, raising the possibility of grip slippage. An alternative design is using fuses directly adhered to FRP specimens. This raises further complications associated with ensuring adequate adhesion strength and further complicates manufacture. A simpler fuse design that is not reliant on extra gripping surfaces was therefore preferred for providing interrupted loading to FRP specimens.

Three criteria were determined to be crucial in the design of an interrupted loading rig for the Instron VHS machine: (i) the load applied to the FRP specimen should be predictable, repeatable, and able to apply a range of loads, (ii) the rig should cause a minimal loss of applied strain rate, and (iii) fuses should be simple to manufacture whilst keeping the overall mass to a minimum. A shear-pin type rig was identified to best fulfil these conditions, with a minimal number of machining operations required per shear pin. The shear pin shown in Figure 1, allows a range of loads to be applied by altering dimension b. Two round grooves were chosen as the preferred pin geometry as it allows a theoretical prediction of the failure strength to be calculated, according to known stress concentration factors for brittle materials [9]. However, initial tests using PMMA shear pins found that the failure load was highly variable. Shear pins were instead manufactured from aluminium 6082-T6, resulting in more repeatable failure loads. Since the aluminium shear pins fail in a ductile manner, the theoretical predictions for brittle materials are not valid and failure loads must be determined experimentally. Shear pins were loaded in series with composite specimens using the rig design shown in **Error! Reference source not found.**. A removable shield was used to prevent the failed shear pin parts being ejected after failure and also to ensure that the notched shear pin sections are in the correct location during loading.

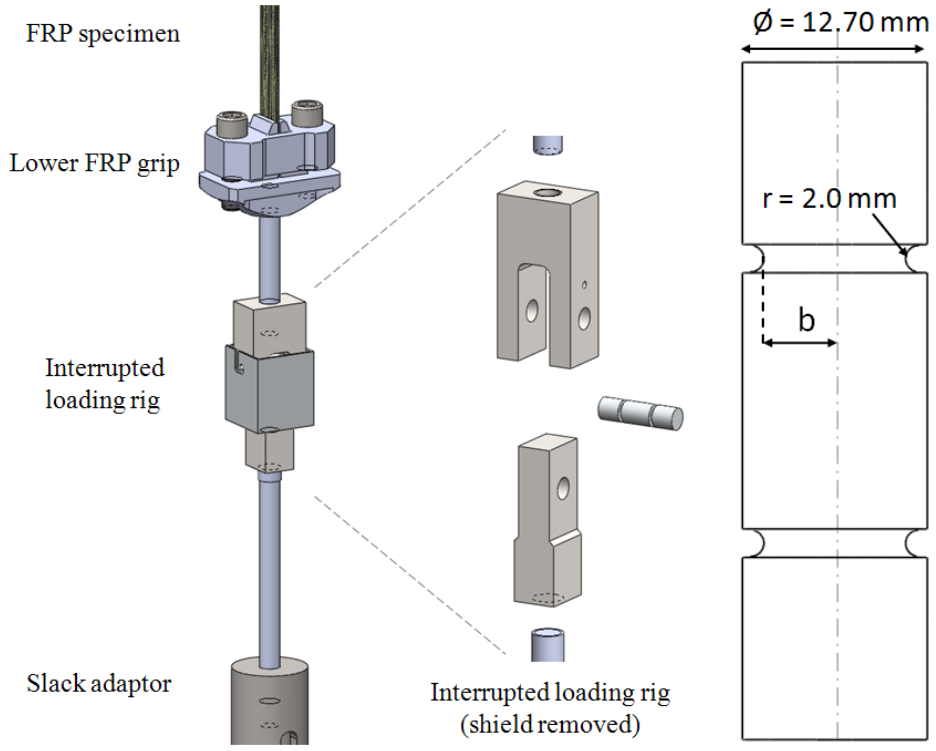

Figure 1. (a) Interruptible loading rig schematic, (b) Shear pin geometry, where dimension b is adjustable according to the failure load required.

3 Anti-Compression Rig Design

Initial trials were carried out using the interrupted loading rig on the Instron VHS in conjunction with high speed white-light imaging at 10 kHz. A selection of such images are shown in Figure 2. It was found that FRP specimens buckled soon after the shear pin failure event. This behaviour was due to the stored elastic energy in the glass fibre reinforced polymer (GFRP) specimen being suddenly released by the shear pin failure. The rig parts still attached to the specimen accelerate upwards, causing the specimen to be loaded under compression due to inertia. A methodology in which compression loading is prevented is required to be certain of the exact cause of any high strain rate damage in FRP specimens.

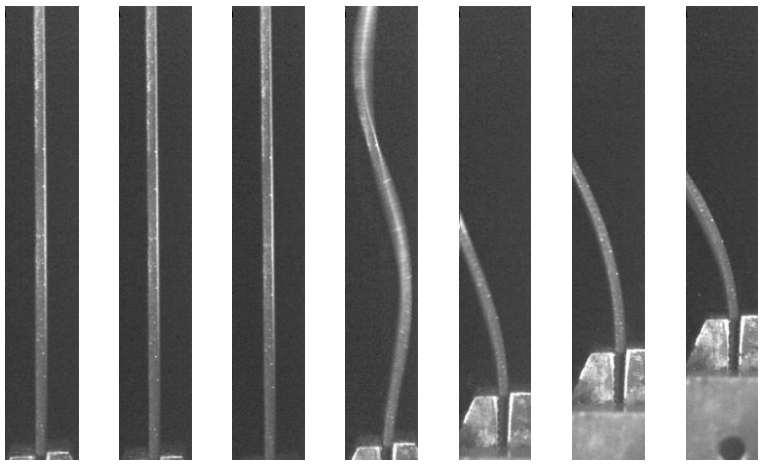

Figure 2. High frequency images of FRP specimen side with interrupted loading rig. Images (a) to (c) show high strain rate tensile loading, whilst images (d) to (g) show specimen buckling after shear pin failure.

Figure 3 shows an additional rig designed to prevent specimens from entering compression. The rig comprises of four M10 threaded struts, a box section crossbeam and a ZX-100EL55 polymer sheet at the point of contact. The rig is situated between the lower FRP grip and the interrupted loading rig, such that upon springback the top surface of the interrupted loading rig impacts with the polymer sheet.

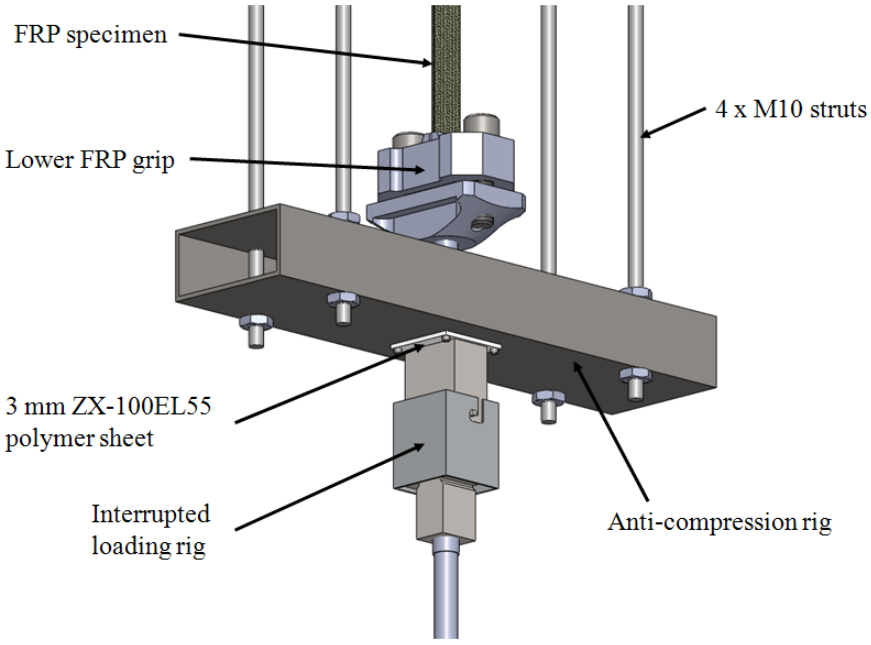

Figure 3. Anti-compression rig design with interrupted loading rig and specimen in situ.

4 Material Characterisation

ACG MTM 28-1 pre-impregnated glass-fibre reinforced epoxy material was used to produce crossply laminates of $[90,0,90,0]_S$ stacking sequence and 1.20 mm thickness. Specimens of 25 mm nominal width and 60 mm gauge length were produced that follow ASTM D 3039 [10]. 40 mm length crossply GFRP end tabs were added to all specimens and bonded using epoxy resin film. 12 specimens were tested to failure using an Instron 5569 electro-mechanical test machine at an extension rate of 2 mm/min (5.56×10^{-4} s^{-1}). The strain was measured using an extensometer of 10 mm gauge length. The mean ultimate tensile stress (UTS) was found to be 513 ± 40 MPa whilst the Young's modulus was found to be 21.22 ± 0.72 GPa.

White-light imaging and DIC were used during the material tests to failure to give an appreciation of the load required to initiate damage. Specimens were coated in three passes of RS matt black paint and once dry, a single light coat of matt white paint was applied to give a speckle pattern. A single LaVision Imager pro LX16M digital camera of 4870 x 3246 pixels, situated perpendicularly to the specimen surface, was used to image the front face of specimens at an imaging frequency of 1 Hz. Illumination was provided by a Schott KL 1500 150-watt cold light source. The commercial DIC software DaVis 7.4 by LaVision was used to process the images. All images were correlated with respect to an image of the specimen under zero load using a cell size of 128 x 128 pixels with 75 % overlap between cells. Figure 4 shows longitudinal strain maps obtained from one specimen using DIC at 25, 50, 75 and 99% of the specimen UTS. It can be seen that bands of high strain develop at higher stress levels. Since the outermost ply is orientated at 90°, such behaviour is likely to be due to transverse cracking, however upon study of the displacement maps no discontinuities could be noted. This could be due to the paint layer being fresh and very ductile, smoothing over any surface cracks, or simply be a characteristic of the material.

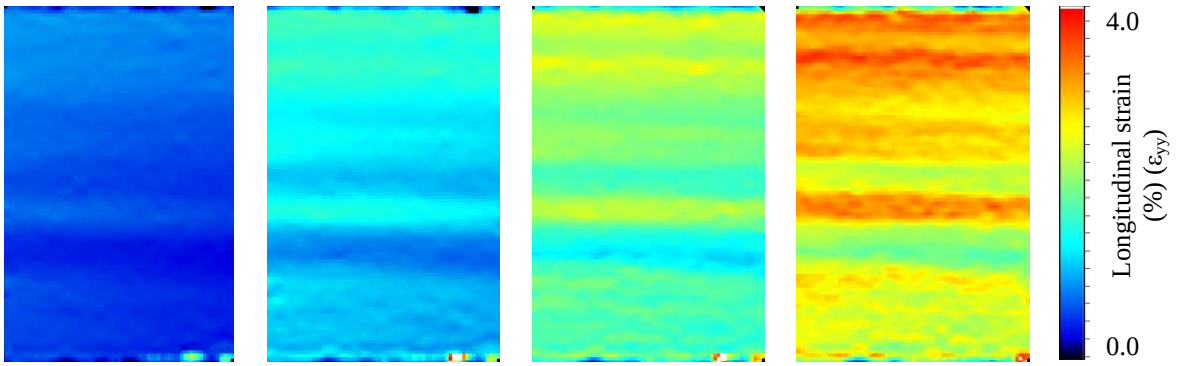

Figure 4. Longitudinal strain maps (ε_{yy}) of a typical $[90,0,90,0]_S$ GFRP specimen obtained through DIC during a quasi-static tensile test to failure.

5 Rig Validation Trials

Based on the DIC strain data shown in Figure 4, a stress level of around 65% of the material UTS was estimated as sufficient to initiate damage in the GFRP specimens using the interrupted loading rig. Shear pins were therefore manufactured with 5.65 ± 0.05 mm minor diameter, failing at around 10 kN, equivalent to 65 % of the specimen UTS. To simplify the initial validation trials, loading was applied using an Instron 5569 electro-mechanical test machine at low strain rates (2.78×10^{-3} s^{-1}). If successful, the methodology can then be transferred to the Instron VHS machine, capable of applying higher strain rate loading. A crucial part of the rig validation is to determine the response after a shear pin has failed and to ensure that FRP specimens do not enter into compression at any point. Two methods were used to measure the specimen response after the shear pin failure event, the first being a strain

gauge situated at the centre of the gauge length and the second being high frequency white-light imaging combined with DIC. A single Vishay CEA-06-240UZ-120 strain gauge was attached to each specimen with the excitation voltage, bridge completion and amplification provided by a Vishay 2311 analogue strain gauge amplifier. A single Photron SA5 high frequency camera, positioned perpendicularly to the specimen surface, was used to record images of the specimen during and after the shear pin failure. The front specimen surface was imaged using a LaVision Imager pro LX16M high resolution digital camera. The speckle pattern applied to the front and back specimen surfaces were adjusted to attempt to account for the differences in spatial resolution between the Imager pro LX16M and the Photron SA5. The front was coated with a fine speckle pattern, whilst coarser speckles were applied to the reverse side by using a larger diameter spray can nozzle.

Data was sampled and synchronised using a PicoScope model 4424 operating at 0.33 MHz. Initial tests were conducted using a small preload on the FRP specimen. This was created by hand tightening the positioning nuts on the four M10 struts such that the crossbeam loads the top of the interrupted loading rig; see Figure 3 for more details. This was intended to prevent the specimen momentarily entering into compression due to rig deformation. The strain gauge response throughout a typical interrupted test is shown in Figure 5 (a). Figure 5 (b) shows the response immediately after shear pin failure. It can be seen that the anti-compression rig prevents the majority of the compression loading previously shown in Figure 2, but does not completely eliminate compression, as shown at 47.92 seconds. To completely eliminate compression loading during an interrupted test, a greater preload was applied by tightening the positioning nuts further to give a pre-strain of 0.62 %. By doing so, the specimen always remained loaded under tension after the shear pin failure event, as shown in Figure 6.

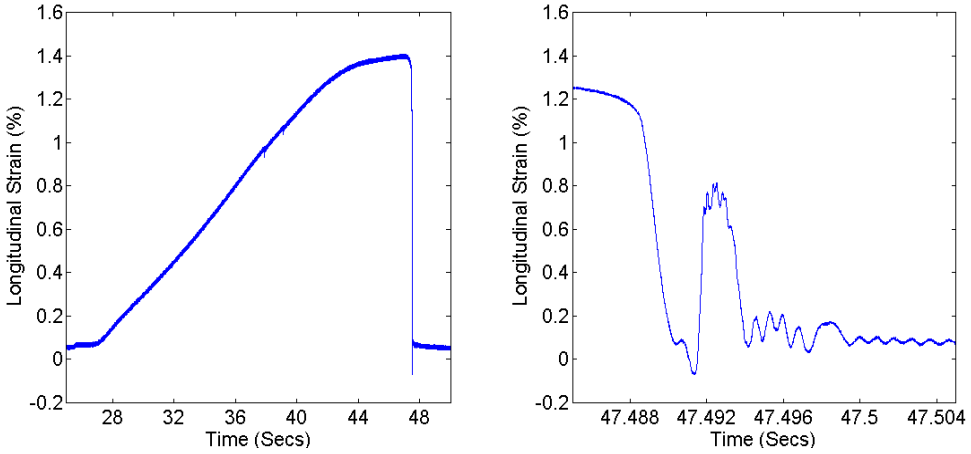

Figure 5. Strain gauge data of a typical interrupted quasi-static test, (a) full test range, (b) strain gauge response just after shear pin failure. Anti-compression rig used with minimal pre-strain on specimen (0.055 % strain).

To further validate the behaviour of the anti-compression rig, the high speed images of the specimen during and after shear pin failure were studied. High speed images were captured at 30 kHz using an exposure time of 1/40000 second. Illumination was provided by a cold light 150 W Fiber-Lite PL900. The camera was set to centre-trigger when the load fell below 2.5 kN. This enabled half of the images before the trigger point and half after the trigger point to be stored. After visual inspection of the images it was found that specimen springback had completely finished before the start of the trigger signal, suggesting a lag in the load cell response. This is unsurprising as the inertia of the load cell and attached grips would delay the load decrease. Due to the limited recording time available, the full test including the initial loading ramp could not be imaged.

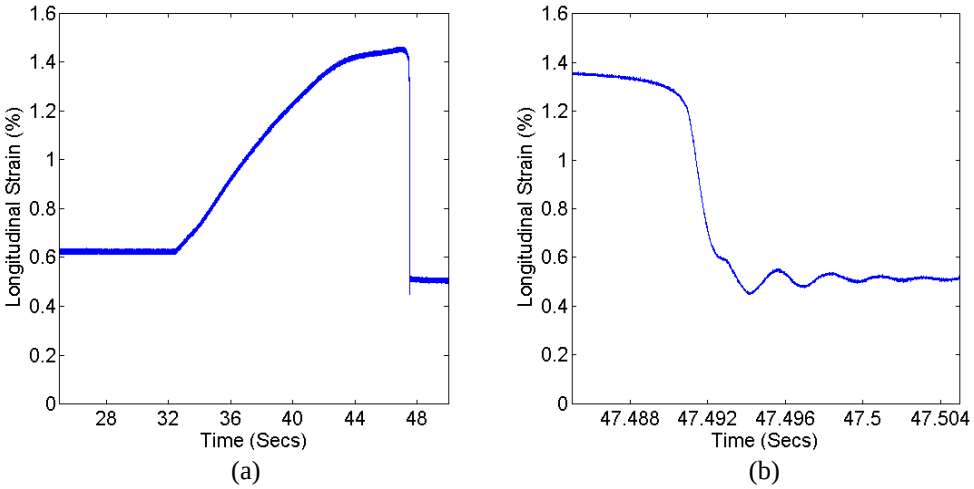

Figure 6. Strain gauge data during a typical interrupted quasi-static test, (a) full test range, (b) strain gauge response just after shear pin failure. Anti-compression rig used with 0.62 % strain preload on specimen.

Images were correlated using the image immediately prior to shear pin failure as the reference image. Therefore all strains calculated are with respect to the point of maximum strain. DIC strain maps were therefore shifted by the maximum strain value registered by the strain gauge, such that the correct strain values can be determined. Image correlations were carried out using a cell size of 64 x 64 pixels with 75 % overlap between cells using DaVis 7.4. A selection of corrected strain maps obtained using DIC are presented in Figure 7. The high speed images collected during the interrupted test were analysed using DIC with strain values corrected by the maximum strain gauge reading. A region of elevated and a region of decreased strain can be noted in the strain maps. These areas correspond to the solder terminals on the strain gauge and the extra terminal blocks. For this reason only the strain map below the strain gauge terminals was deemed reliable. It was found that the minimum strain at any point after the shear pin failure in this area was 0.43 % strain. This compares well with the minimum strain gauge readings and confirms that the specimen does not enter into compression at any point after the failure of the shear pin.

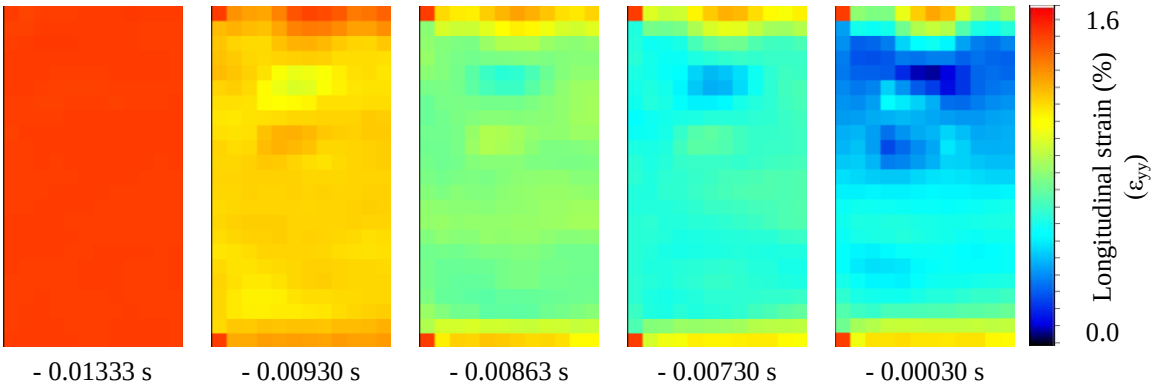

Figure 7. Selection of DIC strain maps from high speed imaging showing specimen response after shear pin failure. Times quoted are with respect to trigger signal time.

The front surface of the specimen was imaged using the LaVision Imager pro LX16M digital camera, with images correlated using a cell size of 128 x 128 pixels with 75 % overlap between cells. The strain maps immediately before and after shear pin failure are shown in Figure 8 (a) and (b) respectively. Bands of transverse cracking can be noted in Figure 8 (a) as expected. The average longitudinal strain in the strain map immediately after shear pin failure is 0.375%. This agrees well with the strain gauge and high speed DIC measurements on the opposite specimen surface.

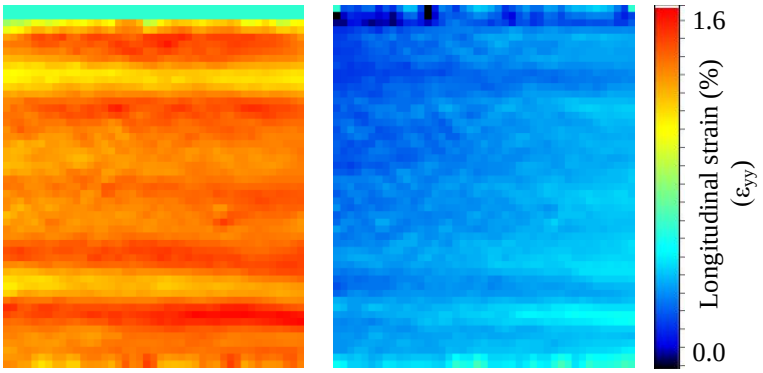

Figure 8. DIC strain maps from front specimen surface imaged with a LaVision Imager pro LX16M camera

6 Conclusions

The tests conducted have successfully validated the use of an aluminium shear pin to provide highly repeatable interrupted loading during low strain rate tests on FRP specimens. The use of an additional rig to prevent specimens entering into compression due to elastic springback has also been validated using both high speed imaging and physical strain gauges. The rig designs are to be adapted to be used with the Instron VHS test machine, so allowing tensile high strain rate interrupted loading to be applied to FRP specimens. A discussion of such tests is to be included in the oral presentation along with initial full-field optical data on the damage initiation response of FRP materials under high strain rate interrupted loading.

Acknowledgements

Many thanks go to LaVision and the Defence Science and Technology Laboratory (Dstl) for loan of camera equipment and to Dstl and the Engineering and Physical Sciences Research Council (EPSRC) for providing the funding for the current research.

References

[1] Pickett A., Fouinneteau M., and Middendorf P. Test and Modelling of Impact on Pre-Loaded Composite Panels. *Applied Composite Materials,* **vol. 16,** pp. 225-244 (2009).
[2] Charca S., Shafiq B., and Just F. Repeated Slamming of Sandwich Composite Panels on Water. *Journal of Sandwich Structures and Materials,* **vol. 11,** pp. 409-424 (2009). September 1, 2009
[3] H. K. and T. K.K. Modeling hail ice impacts and predicting impact damage initiation in composite structures. *AIAA,* **vol. 38,** (2000).
[4] Daniel I.M. and Ishai O., *Engineering Mechanics of Composite Materials*. New York (1994).
[5] Hamouda A.M.S. and Hashmi M.S.J. Testing of composite materials at high rates of strain: advances and challenges. *Journal of Materials Processing Technology,* **vol. 77,** pp. 327-336 (1998).
[6] Daniel I.M., Werner B.T., and Fenner J.S. Strain-rate-dependent failure criteria for composites. *Composites Science and Technology,* **vol. 71,** pp. 357-364 (2011).
[7] Mittelstedt C. and Becker W. Free-Edge Effects in Composite Laminates. *Applied Mechanics Reviews,* **vol. 60,** pp. 217-245 (2007).
[8] Fitoussi J., Meraghni F., Jendli Z., Hug G., and Baptiste D. Experimental methodology for high strain-rates tensile behaviour analysis of polymer matrix composites. *Composites Science and Technology,* **vol. 65,** pp. 2174-2188 (2005).
[9] Pilkey W.D. and Pilkey D.F., *Peterson's Stress Concentration Factors,* Third ed. John Wiley. Hoboken (2008).
[10] ASTM D 3039/D 3039M-95a. *Standard Test Method for Tensile Properties of Polymer Matrix Composite Materials,* (2000).